

# Highly fluorescent water soluble spirobifluorene dye with large Stokes shift: synthesis, characterization and bio-applications

Friederike Schlüter, Kristina Riehemann, Nermin Seda Kehr, Silvio Quici, Constantin G. Daniliuc, Fabio Rizzo\*

## Supporting Information

### Table of Contents

1. General Information
2. Synthesis
3. Crystal structure
4. Photophysical Characterization
5. Fluorescence Microscopy and Cell Viability Assay
6. NMR and Mass Spectra
7. References

### 1. General Information

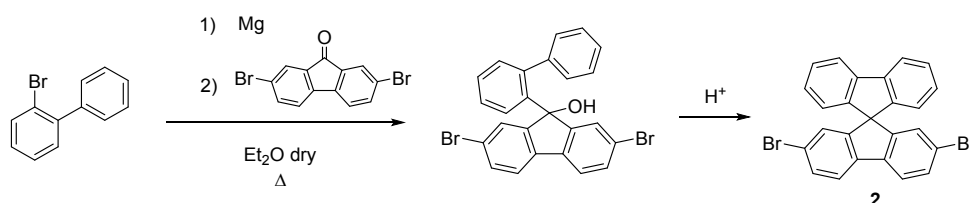
**Chemicals.** All reagents from commercial sources were used without further purification, unless otherwise noted. All dry reactions were performed under Ar atmosphere using glassware that was flamed under high-vacuum and backfilled with Ar. Organic solvents were dried by keeping them over molecular sieves 4A. Column chromatography was carried out on silica gel Si<sub>60</sub>, mesh size 0.040-0.063 mm (Merck, Darmstadt, Germany). Flash chromatography was carried out on silica gel mesh size 230-400 (J. T. Baker) and TLC on aluminum sheets pre-coated with silica gel 60 F254 (E. Merck). <sup>1</sup>H NMR (400 MHz) and <sup>13</sup>C NMR (101 MHz) spectra were obtained with a Bruker Avance 400 spectrometer. Chemical shifts (δ) are given as part per million (ppm) downfield from tetramethylsilane. The assignment of protons and carbon atoms was carried out by bidimensional NMR experiments (COSY, heterocorrelate <sup>1</sup>H-<sup>13</sup>C). The coupling constants *J* are given in Hz. Electrospray ionization (ESI) mass spectroscopy was performed by using a Fourier Transform Ion Cyclotron Resonance (FT-ICR) Mass Spectrometer APEX II and Xmass Software (Bruker Daltonics) at the Centro Interdipartimentale Grandi Apparecchiature (University of Milano).

**X-Ray diffraction:** Data sets for the compound **4** were collected with a D8 Venture Dual Source 100 CMOS diffractometer. Programs used: data collection: APEX2 V2014.5-0;<sup>[S1]</sup> cell refinement: SAINT V8.34A;<sup>[S1]</sup> data reduction: SAINT V8.34A;<sup>[S1]</sup> absorption correction, SADABS V2014/2;<sup>[S1]</sup> structure solution SHELXT-2014;<sup>[S2]</sup> structure refinement SHELXL-2014<sup>[S2]</sup> and graphics, XP.<sup>[S3]</sup> Thermals

ellipsoids are shown with 50% probability. *R*-values are given for observed reflections, and *wR*<sup>2</sup> values are given for all reflections.

**Photophysical experiments.** UV-Vis measurements were performed on a Varian Cary 100 double-beam spectrophotometer and baseline corrected. Extinction molar coefficients were calculated by interpolation of data obtained from 5 solutions. UV-Vis measurements at different temperature were carried out on a Jasco V-650 double-beam spectrophotometer equipped with temperature controller and cooling system, and baseline corrected. Steady-state emission and excitation spectra were recorded on a Fluorolog-3 (Horiba Jobin Yvon) spectrofluorimeter equipped with double-grating monochromator in both the excitation and emission sides, and coupled to a R928P Hamamatsu photomultiplier; a 450 W Xe arc lamp was used as the excitation source. The emission spectra were corrected for detection and optical spectral response of the spectrofluorimeter through a calibration curve supplied by the manufacturer. Fluorescence lifetimes were recorded on a FluoTime300 spectrometer from PicoQuant equipped with two emission monochromators (Czerny-Turner, selectable gratings blazed at 500 nm with 2.7 nm/mm dispersion and 1200 grooves/mm, or blazed at 1250 nm with 5.4 nm/mm dispersion and 600 grooves/mm), Glan-Thompson polarizers for emissions, PMA Hybrid 40 (transit time spread FWHM < 120 ps, 300 –720 nm) as detector and used in TCSPC mode by a PicoHarp 300 (minimum base resolution of 4 ps). Lifetime analysis was performed using the commercial FluoFit software. The quality of the fit was assessed by minimizing the reduced  $\chi^2$  function and visual inspection of the weighted residuals and their autocorrelation. Luminescence quantum yields were measured with a Hamamatsu Photonics absolute PL quantum yield measurement system (C9920-02) equipped with a L9799-01 CW xenon light source (150 W), monochromator, C7473 photonic multichannel analyzer, integrating sphere and employing U6039-05 PLQY measurement software (Hamamatsu Photonics, Ltd., Shizuoka, Japan).

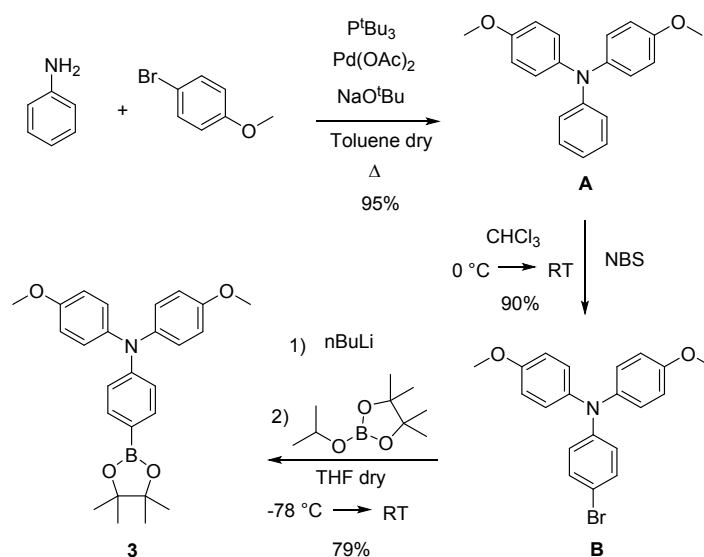
## 2. Synthesis



**Scheme S1.** Synthesis of 2,7-dibromo-9,9'-spirobifluorene (**2**).

**2,7-dibromo-9,9'-spirobifluorene (2).** The spirobifluorene core **2** were synthesized following the procedure reported in literature.<sup>[S4]</sup> 2-Bromobiphenyl (1.65 ml, 9.73 mmol) dissolved in dry Et<sub>2</sub>O (40 ml) was slowly added dropwise to a flask containing Mg (262 mg, 10.76 mmol) under Ar and then refluxed for 4 h to form the corresponding Grignard compound. The solution was added dropwise to a suspension of 2,7-dibromo-9-fluorenone (3.27 g, 9.67 mmol) in dry Et<sub>2</sub>O (70 ml), thus refluxed overnight. After cooling to RT, the reaction was quenched by adding saturated NH<sub>4</sub>Cl aqueous solution (100 ml). After separation of the two phases, the

aqueous phase was extracted with Et<sub>2</sub>O (2 x 30 ml). The collected organic phases were washed with H<sub>2</sub>O (1 x 30 ml) and dried over MgSO<sub>4</sub> before removing the solvent in vacuo. The fluorenol intermediate product crystallized from CH<sub>2</sub>Cl<sub>2</sub>/Hexane mixture as white solid (3.55 g, 7.22 mmol, 75%) was then solubilized in hot glacial acetic acid (50 ml). The addition of few drops of concentrated HCl under stirring induced the precipitation of the desired product as white solid, which was collected by filtration (2.83 g, 83%, 61% overall yield).



**Scheme S2.** Synthesis of 4-(*N,N*-di(4-methoxyphenyl)amino)phenylboronic pinacol ester (**3**).

***N,N*-di(4-methoxyphenyl)aniline (A).** The catalyst was obtained by stirring at RT for 30 minutes Pd(OAc)<sub>2</sub> (74 mg, 0.329 mmol) and P<sup>t</sup>Bu<sub>3</sub> (1M in toluene, 0.53 ml) in dry toluene (1 ml) under Ar in a Schlenk tube. The yellow solution was transferred to a Schlenk tube containing aniline (1.0 ml, 10.95 mmol), 4-bromo-anisole (3.0 ml, 23.96 mmol) and NaO<sup>t</sup>Bu (3.14 g, 32.67 mmol) in dry toluene (12 ml) and refluxed overnight under vigorous stirring. After cooling to RT, saturated NH<sub>4</sub>Cl aqueous solution (20 ml) was added and the phases separated. The aqueous phase was extracted with EtOAc (2 x 20 ml) and dried over MgSO<sub>4</sub> before removing the solvent under vacuum. The crude was purified over silica gel column by eluting with Cyclohexane/EtOAc (10:1) to give the desired product as off-white solid (3.2 g, 95%).

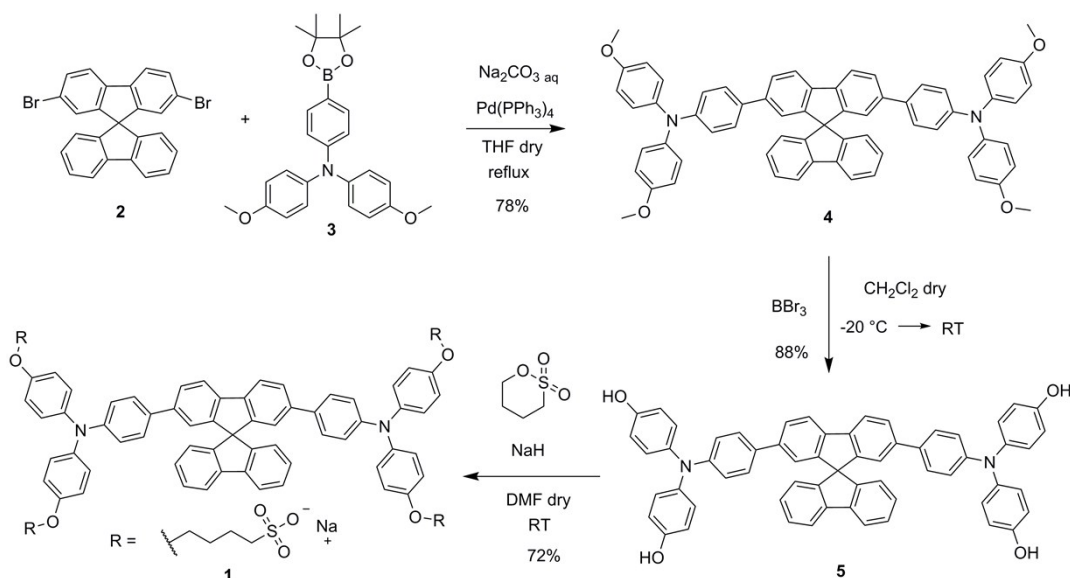
<sup>1</sup>H NMR (300 MHz, CD<sub>2</sub>Cl<sub>2</sub>, 25 °C): 7.19-6.80 (m, 13H, H-phenyl), 3.78 (s, 6H, OCH<sub>3</sub>) ppm.

**4-bromo-*N,N*-di(4-methoxyphenyl)aniline (B).** In a flask **A** (6.71 g, 21.99 mmol) was solubilized in CHCl<sub>3</sub> (30 ml) and cooled to 0 °C with an ice bath. N-bromosuccinimide (NBS) (3.93 g, 22.08 mmol) solubilized in CHCl<sub>3</sub> (30 ml) was added dropwise at 0 °C, afterwards the solution was stirred overnight at RT. The solution was poured in H<sub>2</sub>O (100 ml), thus the phases were separated. The organic phase was dried over MgSO<sub>4</sub> before removing the solvent under vacuum and the crude was purified over silica gel column by eluting with pentane/CH<sub>2</sub>Cl<sub>2</sub> (4:1) to give the product as off-white solid (7.6 g, 90%).

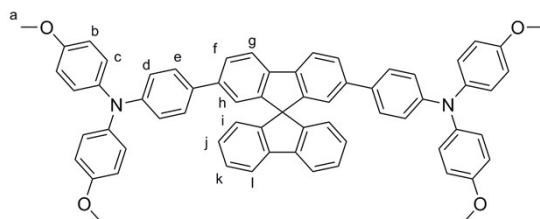
<sup>1</sup>H NMR (300 MHz, CD<sub>2</sub>Cl<sub>2</sub>, 25 °C): 7.23 (d, 2H, J = 8.9 Hz, H-phenyl), 7.03 (d, 4H, J = 9.0 Hz, H-phenyl), 6.83 (d, 4H, J = 9.0 Hz, H-phenyl), 6.76 (d, 2H, J = 8.9 Hz, H-phenyl), 3.77 (s, 6H, OCH<sub>3</sub>) ppm.

**4-(*N,N*-di(4-methoxyphenyl)amino)phenylboronic pinacol ester (**3**)**. In a dried Schlenk **B** (1.00 g, 2.62 mmol) was solubilized in dry THF (25 ml) and cooled to  $-78\text{ }^{\circ}\text{C}$ . *n*BuLi (1.6M in Hexane, 2 ml) was added dropwise and the solution stirred for 1 h at  $-78\text{ }^{\circ}\text{C}$ . 2-isopropoxy-4,4,5,5-tetramethyl-1,3,2-dioxaborolane (0.6 ml, 2.94 mmol) was added to the solution which was stirred at  $-78\text{ }^{\circ}\text{C}$  for additional 2 h, then left stirring overnight at RT. The reaction was poured in  $\text{H}_2\text{O}$  (100 ml) and extracted with  $\text{Et}_2\text{O}$  (2 x 75 ml). The collected organic phases were dried over  $\text{MgSO}_4$  before removing the solvent under vacuum. The crude was purified over silica gel column by eluting with Cyclohexane/ $\text{EtOAc}$  (20:1) to give the desired product as white solid (890 mg, 79%).

$^1\text{H NMR}$  (300 MHz,  $\text{CD}_2\text{Cl}_2$ ,  $25\text{ }^{\circ}\text{C}$ ): 7.52 (d, 2H,  $J = 8.0\text{ Hz}$ , H-phenyl), 7.06-6.80 (m, 10H, H-phenyl), 3.78 (s, 6H,  $\text{OCH}_3$ ), 1.30 (s, 12H,  $\text{CH}_3$ -pinacol) ppm.



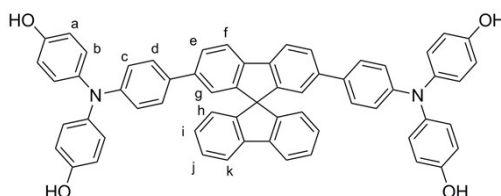
**Scheme 1. Synthesis of 1.**



**2,7-bis(4-[*N,N*-bis(4-methoxyphenyl)amino]phen-1-yl)-9,9'-spirobifluorene (**4**)**. In a Schlenk tube a stirred mixture of **2** (195 mg, 0.411 mmol), **3** (354 mg, 0.826 mmol), aqueous  $\text{Na}_2\text{CO}_3$  1M (1.3 ml) and  $\text{Pd}(\text{PPh}_3)_4$  (27 mg, 0.023 mmol) in dry THF (7 ml) was refluxed overnight under inert atmosphere. After cooling at room temperature, the solvent was removed under reduced pressure, the solid dissolved in  $\text{CH}_2\text{Cl}_2$  and washed with water. The organic phase was dried over  $\text{Na}_2\text{SO}_4$  and the solvent was removed under vacuum. The crude was purified by column chromatography over silica gel using the mixture hexane/ $\text{CH}_2\text{Cl}_2$  (5:1) as eluent to give the product as yellow solid (296 mg, 78%).

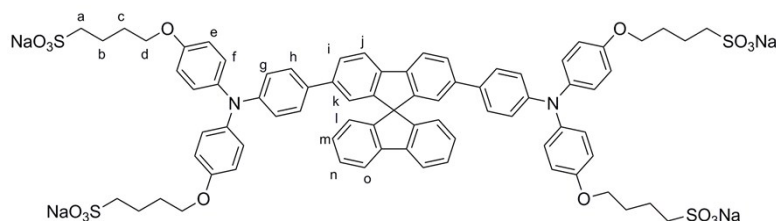
$^1\text{H NMR}$  (400 MHz,  $\text{CD}_2\text{Cl}_2$ ,  $25\text{ }^{\circ}\text{C}$ ): 7.88 (dd, 4H,  $J = 8.0\text{ Hz}$ ,  $\text{H}_g, \text{H}_i$ ), 7.59 (dd, 2H,  $J_1 = 8.0\text{ Hz}$ ,  $J_2 = 1.7\text{ Hz}$ ,  $\text{H}_f$ ), 7.37 (dt, 2H,  $J_1 = 7.5\text{ Hz}$ ,  $J_2 = 0.8\text{ Hz}$ ,  $\text{H}_k$ ), 7.22 (d, 4H,  $J = 8.8\text{ Hz}$ ,  $\text{H}_e$ ), 7.1 (dt, 2H,  $J_1 = 7.5\text{ Hz}$ ,  $J_2 = 0.9$

Hz, H<sub>j</sub>) 6.98 (d, 8H, J = 9.0 Hz, H<sub>b</sub>), 6.85 (d, 2H, J = 1.5 Hz, H<sub>h</sub>), 6.83-6.76 (m, 14H, H<sub>c</sub>, H<sub>d</sub>, H<sub>i</sub>), 3.77 (s, 12H, H<sub>a</sub>) ppm. <sup>13</sup>C NMR (101 MHz, CD<sub>2</sub>Cl<sub>2</sub>, 25 °C): 156.53, 150.32, 149.40, 148.67, 142.40, 141.26, 140.85, 140.62, 133.06, 128.38(C<sub>j</sub>), 128.29 (C<sub>k</sub>), 127.78 (C<sub>e</sub>), 127.03 (C<sub>b</sub>), 126.59 (C<sub>f</sub>), 124.47 (C<sub>i</sub>), 122.16 (C<sub>h</sub>), 121.02 (C<sub>d</sub>), 120.84 (C<sub>g</sub>), 120.64 (C<sub>i</sub>), 115.12 (C<sub>c</sub>), 66.60 (C spiro), 55.95 (C<sub>a</sub>) ppm. *m/z* (HRMS ESI<sup>+</sup>): 922.3751 (M<sup>+</sup>. C<sub>65</sub>H<sub>50</sub>N<sub>2</sub>O<sub>4</sub> requires 922.3765), 461.1884 (M<sup>2+</sup>. C<sub>65</sub>H<sub>50</sub>N<sub>2</sub>O<sub>4</sub> requires 461.1880).



**2,7-bis(4-[N,N-bis(4-hydroxyphenyl)amino]phen-1-yl)-9,9'-spirobifluorene (5).** In a three-neck flask **4** (120.3 mg, 0.130 mmol) was solubilized in dry CH<sub>2</sub>Cl<sub>2</sub> (10 ml) under inert atmosphere and cooled at -20 °C. After the addition of BBr<sub>3</sub> (1M in CH<sub>2</sub>Cl<sub>2</sub>, 0.79 ml), the stirring solution was kept at -20 °C for one hour, then left to come to room temperature overnight under stirring. On the morning the solution was poured in H<sub>2</sub>O (20 ml) and the aqueous phase extracted with ethyl acetate until the organic phase was colorless. The collected organic phases were dried over Na<sub>2</sub>SO<sub>4</sub> and the solvent removed under vacuum. The crude was purified by column chromatography using CH<sub>2</sub>Cl<sub>2</sub>/MeOH (96:4) as eluent to give the product as green solid (100.0 mg, 88%).

<sup>1</sup>H NMR (400 MHz, CD<sub>3</sub>OD, 25 °C): 7.74 (d, 2H, J = 8.0 Hz, H<sub>k</sub>), 7.73 (d, 2H, J = 7.4 Hz, H<sub>f</sub>), 7.38 (d, 2H, J = 8.0 Hz, H<sub>e</sub>), 7.16 (t, 2H, J = 7.4 Hz, H<sub>j</sub>), 6.91 – 6.85 (m, 6H, H<sub>i</sub>, H<sub>d</sub>), 6.76 (d, 8H, J = 8.7 Hz, H<sub>a</sub>), 6.62 – 6.57 (m, 14H, H<sub>b</sub>, H<sub>c</sub>, H<sub>g</sub>), 6.48 (d, 2H, J = 7.6 Hz, H<sub>h</sub>) ppm. <sup>13</sup>C NMR (101 MHz, CD<sub>3</sub>OD, 25 °C): 154.70, 150.96, 150.23, 149.65, 142.99, 141.67, 141.20, 133.20, 128.99 (C<sub>j</sub>), 128.96 (C<sub>i</sub>), 128.06 (C<sub>d</sub>), 127.98 (C<sub>a</sub>), 127.12 (C<sub>e</sub>), 125.03 (C<sub>h</sub>), 122.32 (C<sub>g</sub>), 121.35 (C<sub>k</sub>), 121.17 (C<sub>f</sub>), 121.01 (C<sub>c</sub>), 117.01 (C<sub>b</sub>), 67.32 (C spiro) ppm.



**Tetrasodium 2,7-bis(4-(N,N-bis[4-(3-sulfonatobutoxy)]phenyl)amino)phen-1-yl)-9,9'-spirobifluorene (1).** In a dried two-neck flask NaH 60% (75.5 mg, 1.89 mmol) was first washed with pentane (2 x 8 ml) and then, after the removal of the solvent, suspended in dry DMF (20 ml). **5** (65.7 mg, 0.0758 mmol) dissolved in dry DMF (20 ml) was added to the suspension under inert atmosphere and stirred vigorously for 1 hour. Then 1,4-butane sultone (0.05 ml, 0.490 mmol) was added and the mixture was stirred vigorously overnight. The little amount of precipitate was filtered off after washing with DMF and the volume reduced under vacuum until circa 10 ml. CH<sub>2</sub>Cl<sub>2</sub> (circa 150 ml) was added to induce precipitation. After filtration, the solid was washed with CH<sub>2</sub>Cl<sub>2</sub> and the product was purified by precipitation from MeOH and ethyl acetate (82.1 mg, 72%).

<sup>1</sup>H NMR (400 MHz, CD<sub>3</sub>OD, 25 °C): 7.93 (d, 2H, J = 7.6 Hz, H<sub>o</sub>), 7.92 (d, 2H, J = 8.1 Hz, H<sub>j</sub>), 7.60 (d, 2H, J = 8.2 Hz, H<sub>i</sub>), 7.38 (t, 2H, J = 7.5 Hz, H<sub>n</sub>), 7.20 (d, 4H, J = 8.5 Hz, H<sub>h</sub>), 7.14 (t, 2H, J = 7.5 Hz, H<sub>m</sub>), 6.94 (d, 8H,

J = 9.0 Hz, H<sub>e</sub>), 6.83 – 6.79 (m, 12H, H<sub>f</sub>, H<sub>g</sub>), 6.75 – 6.71 (m, 4H, H<sub>k</sub>, H<sub>l</sub>), 3.96 (t, 8H, J = 6.0 Hz, H<sub>d</sub>), 2.87 (t, 8H, J<sub>1</sub> = 7.3, J<sub>2</sub> = 7.9, H<sub>a</sub>), 2.00 – 1.85 (m, 16H, H<sub>b</sub>, H<sub>c</sub>) ppm. <sup>13</sup>C NMR (101 MHz, CD<sub>3</sub>OD, 25 °C): 155.45, 149.69, 148.16, 141.75, 140.72, 140.43, 139.97, 132.51, 127.59 (C<sub>n</sub>), 127.58 (C<sub>m</sub>), 126.75 (C<sub>h</sub>), 126.18 (C<sub>e</sub>), 125.82 (C<sub>i</sub>), 123.53 (C<sub>l</sub>), 120.95 (C<sub>k</sub>), 120.30 (C<sub>g</sub>), 119.94 (C<sub>o</sub>), 119.80 (C<sub>j</sub>), 114.99 (C<sub>f</sub>), 67.47 (C<sub>d</sub>), 50.95 (C<sub>a</sub>), 28.12 (C<sub>b</sub>), 21.57 (C<sub>c</sub>) ppm.

*m/z* (HRMS ESI<sup>+</sup>): 351.5907 (M<sup>4+</sup>. C<sub>77</sub>H<sub>70</sub>N<sub>2</sub>O<sub>16</sub>S<sub>4</sub> requires 351.5907), 476.4509 (M<sup>3+</sup>. C<sub>77</sub>H<sub>70</sub>N<sub>2</sub>O<sub>16</sub>S<sub>4</sub>Na requires 476.4507), 726.1724 (M<sup>2+</sup>. C<sub>77</sub>H<sub>70</sub>N<sub>2</sub>O<sub>16</sub>S<sub>4</sub>Na<sub>2</sub> requires 726.1707).

### 3. Crystal structure

**X-ray crystal structure analysis of 4:** A pale yellow prism-like specimen of C<sub>65</sub>H<sub>50</sub>N<sub>2</sub>O<sub>4</sub>, approximate dimensions 0.030 mm x 0.049 mm x 0.231 mm, was used for the X-ray crystallographic analysis. The X-ray intensity data were measured. A total of 839 frames were collected. The total exposure time was 19.81 hours. The frames were integrated with the Bruker SAINT software package using a narrow-frame algorithm. The integration of the data using a monoclinic unit cell yielded a total of 52300 reflections to a maximum  $\theta$  angle of 25.03° (0.84 Å resolution), of which 8385 were independent (average redundancy 6.237, completeness = 99.9%, R<sub>int</sub> = 12.89%, R<sub>sig</sub> = 11.35%) and 5434 (64.81%) were greater than 2 $\sigma$ (F<sup>2</sup>). The final cell constants of  $\underline{a}$  = 14.9397(9) Å,  $\underline{b}$  = 9.2935(5) Å,  $\underline{c}$  = 34.6459(18) Å,  $\beta$  = 98.609(2)°, volume = 4756.1(5) Å<sup>3</sup>, are based upon the refinement of the XYZ-centroids of 9938 reflections above 20  $\sigma$ (I) with 4.541° < 2 $\theta$  < 55.03°. Data were corrected for absorption effects using the multi-scan method (SADABS). The ratio of minimum to maximum apparent transmission was 0.756. The calculated minimum and maximum transmission coefficients (based on crystal size) are 0.9820 and 0.9980. The structure was solved and refined using the Bruker SHELXTL Software Package, using the space group *P*2<sub>1</sub>/*n*, with Z = 4 for the formula unit, C<sub>65</sub>H<sub>50</sub>N<sub>2</sub>O<sub>4</sub>. The final anisotropic full-matrix least-squares refinement on F<sup>2</sup> with 739 variables converged at R<sub>1</sub> = 9.91%, for the observed data and wR<sub>2</sub> = 16.04% for all data. The goodness-of-fit was 1.186. The largest peak in the final difference electron density synthesis was 0.294 e<sup>-</sup>/Å<sup>3</sup> and the largest hole was -0.276 e<sup>-</sup>/Å<sup>3</sup> with an RMS deviation of 0.066 e<sup>-</sup>/Å<sup>3</sup>. On the basis of the final model, the calculated density was 1.289 g/cm<sup>3</sup> and F(000), 1944 e<sup>-</sup>.

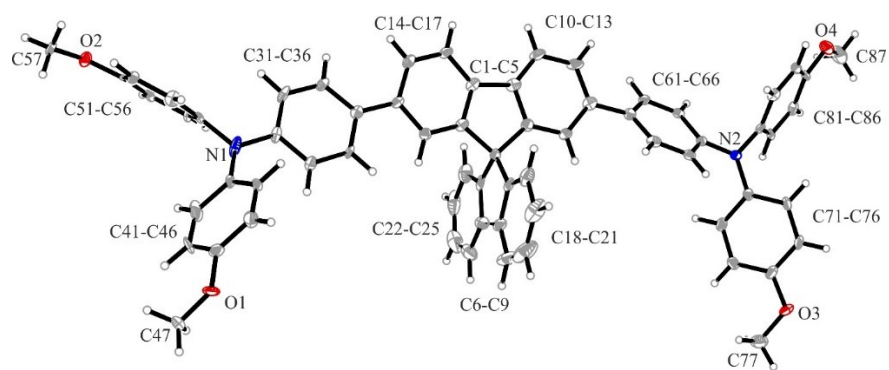
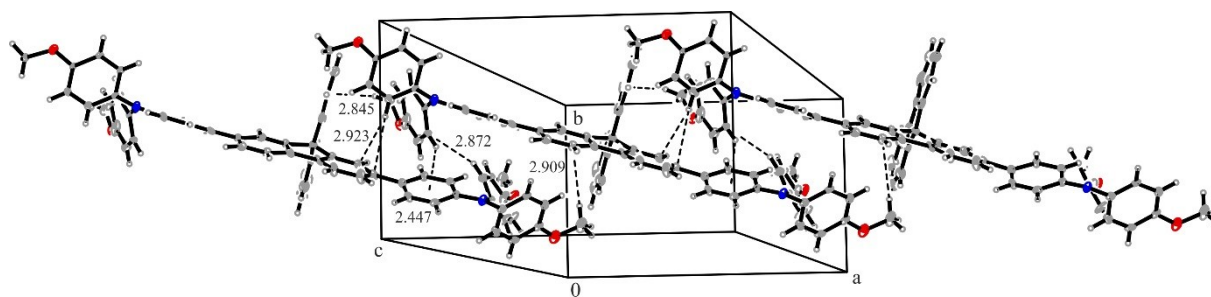
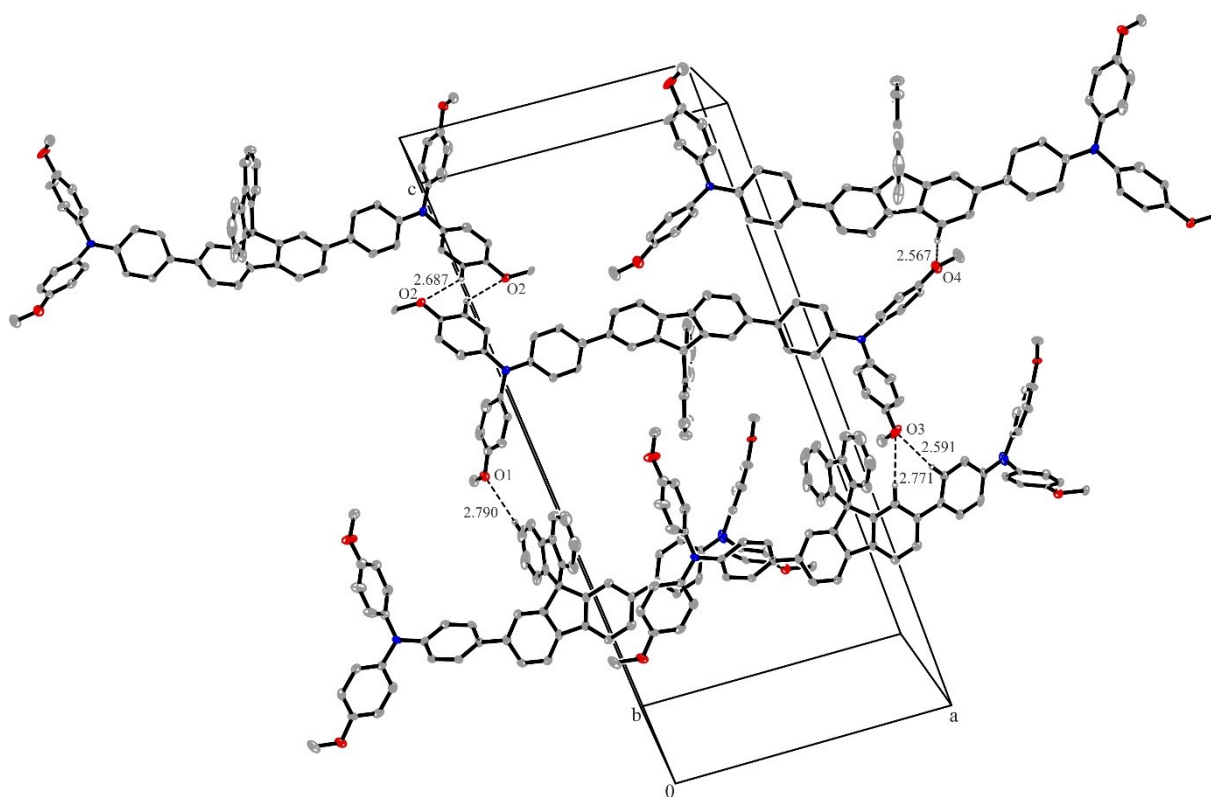


**Figure S1.** Crystal structure of compound **4**. Thermal ellipsoids are shown at 50% probability



(A)



(B)

**Figure S2.** Excerpt of packing diagram of compound **4** presenting non-covalent interactions. (A) CH $\cdots$  $\pi$  interactions along the *a*-axis, (B) CH $\cdots$ O interactions involving all four methoxy groups in **4**. Only the involved hydrogen atoms are shown.

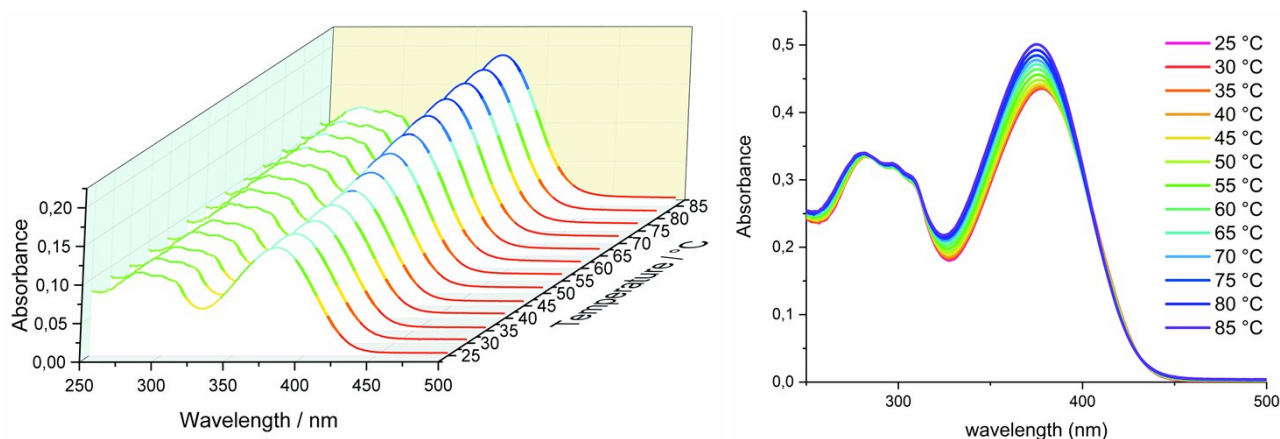
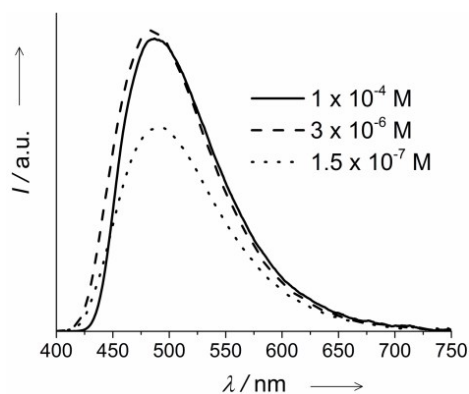
**Table S1.** Non-covalent intermolecular interactions CH...O and CH... $\pi$  in compound **1** (Å and deg)<sup>a</sup>

D-H...A	d(D-H)	d(H...A)	d(D...A)	$\angle(DHA)$
C53-H53...O2 <sup>#1</sup>	0.95	2.687	3.421	134.6
C23-H23...O1 <sup>#2</sup>	0.95	2.790	3.603	144.0
C14-H14...O3 <sup>#3</sup>	0.95	2.771	3.705	168.0
C36-H36...O3 <sup>#3</sup>	0.95	2.590	3.300	131.7
C17-H17...O4 <sup>#4</sup>	0.95	2.566	3.434	151.9
C42-H42...Cg <sup>#5, a</sup>	0.95	2.477	3.301	144.9
C46-H46...Cg <sup>#6, b</sup>	0.95	2.883	3.741	150.9
C47-H47...Cg <sup>#7, c</sup>	0.98	2.678	3.461	137.2
C56-H56...Cg <sup>#5, d</sup>	0.95	2.877	3.819	171.0
C57-H57...Cg <sup>#8, e</sup>	0.95	2.661	3.621	166.2
C83-H83...Cg <sup>#9, f</sup>	0.95	2.635	3.576	155.7
C76-H76...Cg <sup>#10, g</sup>	0.95	2.887	3.719	146.9
C87-H87...Cg <sup>#10, h</sup>	0.98	2.957	3.862	154.0

<sup>a</sup> Symmetry transformations used to generate equivalent atoms: <sup>#1</sup> -x, -y+2, -z+1; <sup>#2</sup> -x+1/2, y-1/2, -z+1/2; <sup>#3</sup> -x+3/2, y-1/2, -z+1/2; <sup>#4</sup> -x+2, -y, -z+1; <sup>#5</sup> x-1, y-1, z; <sup>#6</sup> x-1, y+1, z; <sup>#7</sup> -x+1/2, y+1/2, -z+1/2; <sup>#8</sup> -x+1, -y+1, -z+1; <sup>#9</sup> x+1, y-1, z; <sup>#10</sup> x+1, y, z; <sup>a</sup> Cg is the ring centroid of atoms C61/C62/C63/C64/C65/C66; <sup>b</sup> Cg is the centroid of atoms C65/C66; <sup>c</sup> Cg is the ring centroid of atoms C6/C7/C18/C19/C20/C21; <sup>d</sup> Cg is the centroid of atoms C12/C13; <sup>e</sup> Cg is the centroid of atoms C82/C83/C84; <sup>f</sup> Cg is the centroid of atoms C31/C32/C33; <sup>g</sup> Cg is the centroid of atoms C42/C43; <sup>h</sup> Cg is the centroid of atoms C5/C17.

## 4. Photophysical Characterization

### Investigation of aggregates formation

**Figure S3.** Absorption spectra of **1** in H<sub>2</sub>O (left  $3 \times 10^{-6}$  M, right  $1 \times 10^{-4}$  M) at different temperature (from 25 to 85 °C).**Figure S4.** Emission spectra of **1** at different concentrations. The  $\lambda_{\max}$  are 483, 480 and 494 nm at  $1 \times 10^{-4}$  M,  $3 \times 10^{-6}$  M and  $1.5 \times 10^{-7}$  M, respectively, with  $\lambda_{\text{exc}} = 378$  nm.

## Viscosity experiments

**Table S2.** Summary of viscosity experiment data.

MeOH/glycerol	Viscosity (cP)	Abs (nm)	Emission (nm)	Lifetime (ns)	Chi2
10:0	0.54	379	487	2.74 (93%) 0.08 (7%)	0.987
9:1	1.1	379	488	2.88 (98%) 0.17 (2%)	1.049
7:3	5.1	380	492	2.98 (98%) 0.27 (2%)	1.041
5:5	22.5	382	492	3.00 (94%) 0.88 (4%) 0.12 (2%)	1.013
3:7	100.0	383	492	2.92 (90%) 0.92 (7%) 0.17 (3%)	0.985
1:9	443.2	385	484	2.86 (74%) 1.26 (17%) 0.39 (8%)	0.988

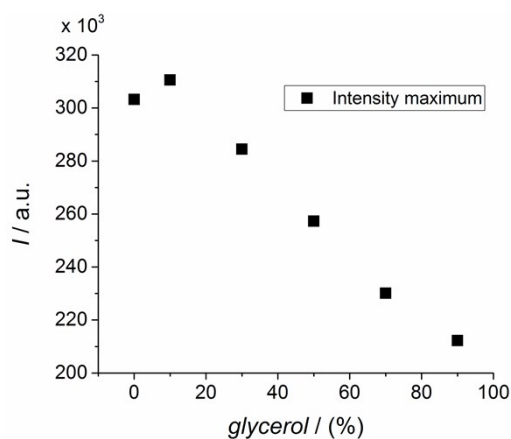


**Figure S5.** Change of the intensity emission with the concentration of glycerol.

## Effect of pH on photophysical properties of the free dye 1

The measurements were performed by solubilizing **1** in solution with different pH: aqueous HCl (pH 2.4), acetate buffer (pH 3.8), phosphate buffer (pH 5.9), phosphate buffer (pH 8.1), aqueous NaOH (pH 12.2).

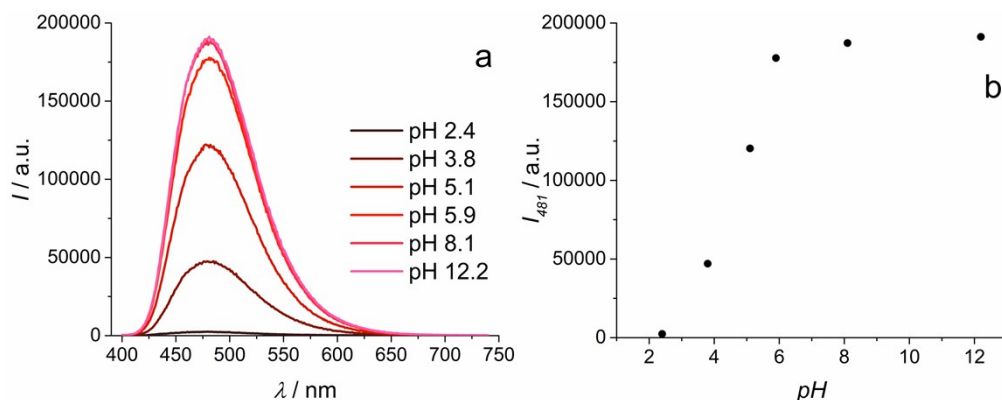


**Figure S6.** a) PL of **1** recorded at different pH (3  $\mu$ M,  $\lambda_{\text{exc}}$  = 378 nm); b) change of the intensity at PL maximum vs. pH.

### Interaction with BSA

Two stock solutions of BSA (3.00  $\times 10^{-5}$  M) and of **1** (1.00  $\times 10^{-4}$  M) in PBS (pH 7.2) was prepared and the aliquots of biomolecule stock solutions were incubated with 3  $\mu$ M solution of **1** in a total volume of 3 ml for each probe for absorption and emission experiments.

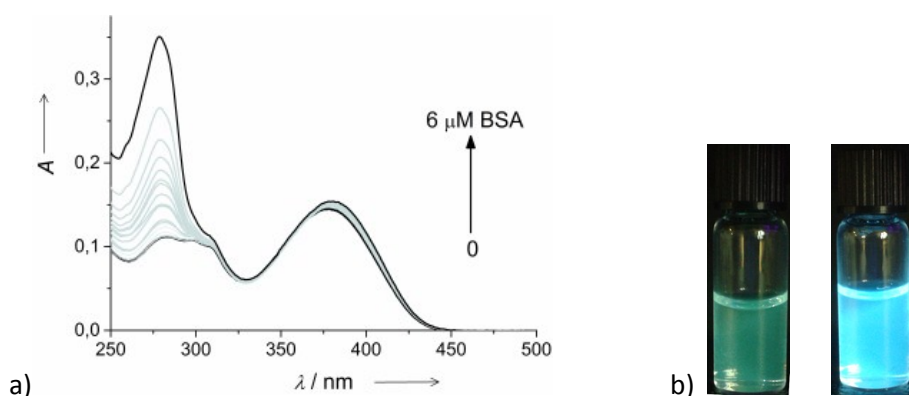


**Figure S7.** Effect of the presence of BSA in aqueous solution of **1** (3  $\mu$ M) a) in absorption, b) under common UV laboratory lamp (left: without protein; right: with BSA (0.8  $\mu$ M)).

### Calculation of the detection limit

The detection limit (or limit of detection, LOD) was calculated using the formula:

$$LOD = S/N \frac{\sigma}{s}$$

where  $S/N$  is the signal-to-noise ratio (= 3),  $\sigma$  the standard deviation of the blank solution and  $s$  the slope of the calibration curve. The standard deviation was obtained measuring 10 independent samples of **1** (3  $\mu$ M) as blank and calculating the corresponding standard deviation. The calibration curve is obtained measuring the fluorescence intensity at different concentration of BSA and  $s$  is the slope obtained fitting the points in the linear range.

**Table S3.** Summary of photophysical data of **1** in different local environment.

solvent <sup>[a]</sup>	Abs nm	PL <sup>[b]</sup> nm	Stokes shift cm <sup>-1</sup> (nm)	fwhm cm <sup>-1</sup>
PBS	378	480	5620 (102)	3610
PBS with BSA	378	461	4760 (83)	3210
Triton X-100	385	462	4280 (77)	3580
SDS	378	477	5490 (99)	3670
CTAB	382	492	5850 (110)	3890
Tween 20	385	476	4970 (91)	3680

[a] Measurements performed using 3  $\mu$ M of **1**. [b] Recorded exciting at 378 nm.

## Binding Constant Evaluation

### Stern-Volmer Analysis

Two stock solutions of BSA ( $3.00 \times 10^{-5}$  M) and of **1** ( $1.00 \times 10^{-4}$  M) in PBS (pH 7.2) were prepared and the aliquots of dye stock solutions were incubated with 2.5  $\mu$ M solution of BSA in a total volume of 3 ml for each probe for absorption and emission experiments.

The quenching of the BSA emission can be described by the standard Stern-Volmer equation

$$I_0/I = 1 + K_{SV}[Q] = 1 + k_q\tau_0[Q]$$

where  $I_0$  and  $I$  are respectively the fluorescence intensities in the absence and presence of **1**,  $K_{SV}$  is the Stern-Volmer quenching constant,  $k_q$  is the bimolecular quenching rate constant,  $\tau_0$  is the average lifetime of BSA without the quencher ( $= 1 \times 10^{-8}$  s)<sup>[S5]</sup> and  $[Q]$  is the concentration of **1**. The  $I$  values have been corrected by the inner filter effect.<sup>[S5]</sup>

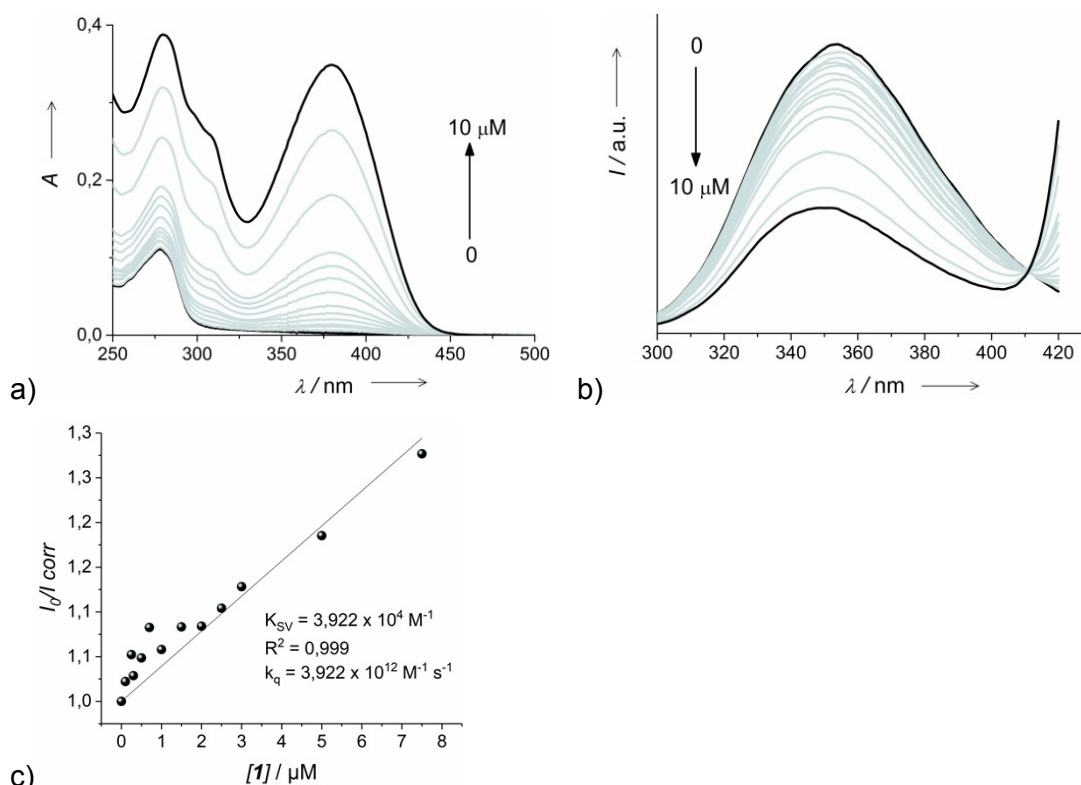


**Figure S8.** Absorption (a) and corrected emission (b,  $\lambda_{exc} = 280$  nm) spectra of BSA (2.5  $\mu\text{M}$ ) at different concentration of **1** (0-10  $\mu\text{M}$ ); c) Stern-Volmer plot.

### Fit of fluorescence data

Different formula were used to fit the fluorescence data of **1** (3  $\mu\text{M}$ ) in presence of different concentration of BSA (0-6  $\mu\text{M}$ ). From the Hill equation (eq. 1, Figure S9a) we obtained the value of number of binding sites ( $n$ ) and dissociation constant ( $K_d$ ), from which we calculated the binding constant ( $K_a$ ):

$$y = I_{max} * \frac{x^n}{(K_d^n + x^n)} \quad (\text{eq. 1})$$

The other two formula are reciprocal fitting<sup>[S6]</sup> (eq. 2) and Benesi-Hildebrand fitting (eq. 3), giving in both case a linear behavior:

$$\frac{(I_{max} - I_0)}{(I - I_0)} = 1 + (K_a * [BSA])^{-1} \quad (\text{eq. 2})$$

$$\frac{1}{(I - I_0)} = \frac{1}{(I_{max} - I_0)} + \frac{1}{K_a(I_{max} - I_0)[BSA]} \quad (\text{eq. 3})$$

Where  $I_0$  is the intensity in absence of BSA,  $I$  is the intensity in the presence of BSA,  $I_{max}$  is the intensity upon saturation and  $K_a$  is the binding constant.

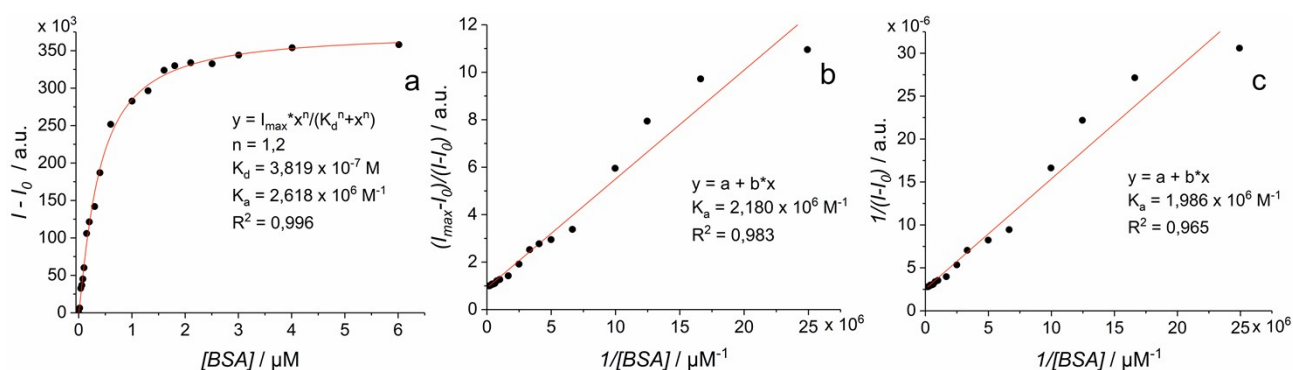


**Figure S9.** Different fitting of fluorescence data of **1** in presence of BSA.

### Interaction with other proteins

Stock solutions of BSA ( $3.00 \times 10^{-5} \text{ M}$ ), pepsin ( $2.00 \times 10^{-5} \text{ M}$ ), protamine sulfate ( $1.00 \times 10^{-4} \text{ M}$ ), horseradish peroxidase (HRP,  $2.00 \times 10^{-5} \text{ M}$ ) and of **1** ( $1.00 \times 10^{-4} \text{ M}$ ) in PBS (pH 7.2) were prepared. Aliquots of biomolecule stock solutions ( $1 \mu\text{M}$ ) were incubated with  $3 \mu\text{M}$  solution of **1** in a total volume of 3 ml for each probe for absorption and emission experiments.

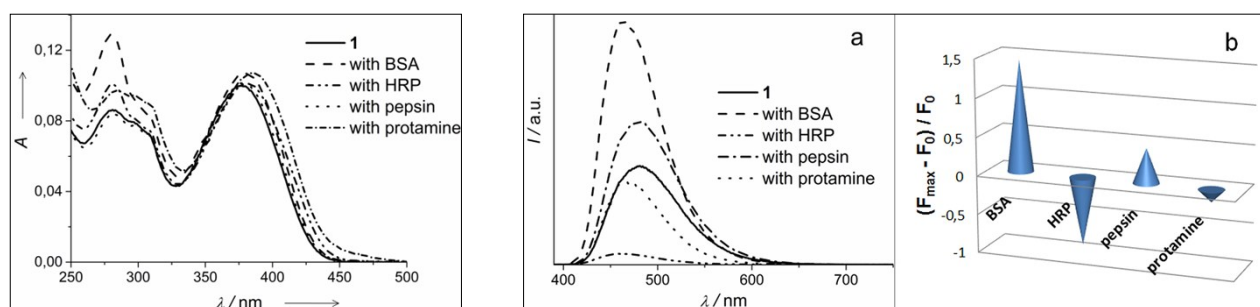


**Figure S10.** Absorption spectra (left) of **1** in presence of different proteins ( $1 \mu\text{M}$ ); PL spectra (right,  $\lambda_{\text{exc}} = 378 \text{ nm}$ ) of **1** ( $3 \mu\text{M}$ , PBS): a) with different proteins ( $1 \mu\text{M}$ ), b) variations on the intensity depending on the proteins.

### Selective-site determination in **1**:BSA binary system

Stock solutions of **1**:BSA ( $3:1 \mu\text{M}$ ) in water, dansylamide (DNSA) and Ibuprofen in DMSO ( $3 \text{ mM}$ ) were prepared. The dye:protein solution was divided in two parts. PL intensity was measured after successive addition of competitive ligand for every solution. The displacement was calculated by using the following formula:

$$\text{displacement}(\%) = (I_0/I - 1) * 100$$

## pH effect on 1:BSA binary system

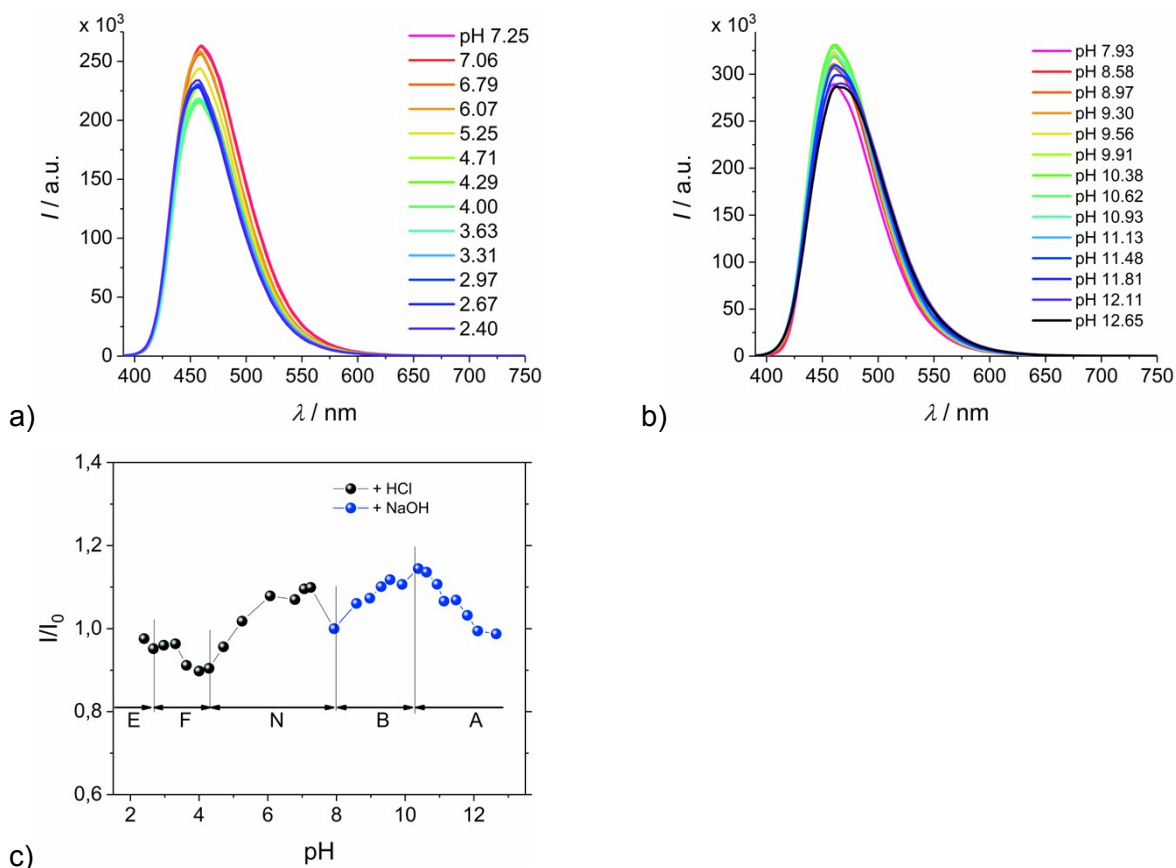


**Figure S11.** Effect of pH on the PL of 1:BSA complex in acidic (a) and basic (b) condition. c) variation of PL intensity in relationship with the BSA isomers (E = extended, F = fast, N = normal, B = basic, A = aged).

## CD spectroscopy

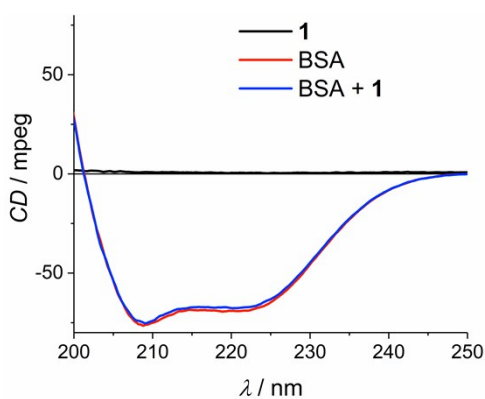


**Figure S12.** Investigation of 1:BSA complex in water by circular dichroism (CD) spectroscopy.

## Surfactants

Stock solutions of **1** ( $1.50 \times 10^{-4}$  M) in surfactants were prepared by dissolving the dye in the aqueous solution of surfactant at the critical micelle concentration (cmc). Aliquots of the stock

solutions (60  $\mu$ l) were diluted in a total volume of 3 ml to have 3  $\mu$ M as final concentration for absorption and emission experiments.

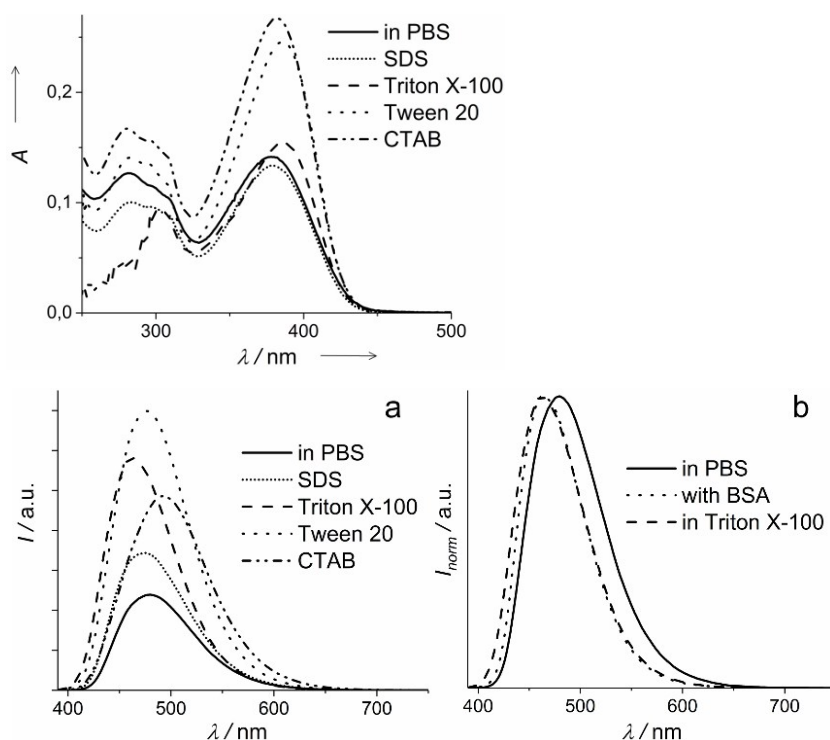


**Figure S13.** Top: Absorption spectra of **1** (3  $\mu$ M) in different surfactants. Below: PL spectra ( $\lambda_{exc} = 378$  nm) of **1** (3  $\mu$ M, PBS): a) in different surfactants, b) normalized PL.

## 5. Fluorescence Microscopy and Cell Viability Assay

### Cell Culture and Fluorescence Microscopy

The primary dermal fibroblast cells (ATCC, USA) were cultured in fibroblast basal medium supplemented with fibroblast growth kit low serum (ATCC, USA). Human Umbilical Vein Endothelial cells (HUVECs; ATCC, USA) were cultured in Endothelial Cell Growth Medium.

Macrophages were isolated from buffycoats of the peripheral blood obtained from the Red Cross taken from healthy volunteers. Briefly, mononuclear cells were prepared via Ficoll gradient centrifugation followed by subsequent isolation of CD14 positive cells by magnetic associated cell sorting (MACS, Miltenyi Biotec GmbH, Bergisch Gladbach, Germany). The purity of at least 95% of positive cells was determined by flow cytometry in an Agilent 2100 Bioanalyzer (Agilent Technologies Deutschland GmbH, Waldbronn, Germany).

The cells were incubated at 37° C and 5% CO<sub>2</sub> in a humidified atmosphere. For microscopically analysis cell were cultured on coverslips and incubated for 24h hours with substance **1** (1  $\mu$ M or 50  $\mu$ M), subsequently followed by microscopically analysis with a fluorescence microscope (Nikon Instruments Europe B. V., Germany).

### Cell Viability XTT Assay

The cells were cultured as described above. The cell viability assay (XTT, Sigma-Aldrich Chemie GmbH, Munich, Germany) was applied according to the manufacturers protocol. Briefly, cells were seeded in a 96 well plate. For the test cells were incubated for 18 h with substance **1** (1  $\mu\text{M}$  and 50  $\mu\text{M}$ ), for solvent control for the same time with 10  $\mu\text{L}$   $\text{H}_2\text{O}$ . For positive control cells were incubated for 0.5 h with 60  $\mu\text{g/ml}$  Digitonin. Absorbance was measured using a microplate reader (FluoStar Optima, Agilent Technologies, Santa Clara, USA). For evaluation, cell viability was determined as percentage of the negative control. Digitonin served as positive control, water solvent as negative control, respectively.

Our results indicate that the viability of the investigated primary cells is not influenced by the uptake of molecule **1** even at high concentration. However, additionally viability experiment performed by using Neubauer chamber confirmed that **1** has no cytotoxic effect. Moreover, fluorescence microscopy images of living primary dermal Fibroblast, HUVEC and macrophages cells incubated with higher concentrated solution of **1** (50  $\mu\text{M}$ ) display the same visualization as previously shown in Figure 4 (see Figure S14a). The pictures of unstained living primary dermal Fibroblast cell recorded with bright field and with blue filter (DAPI) (Figure S14b) show that the autofluorescence of the cell is negligible.

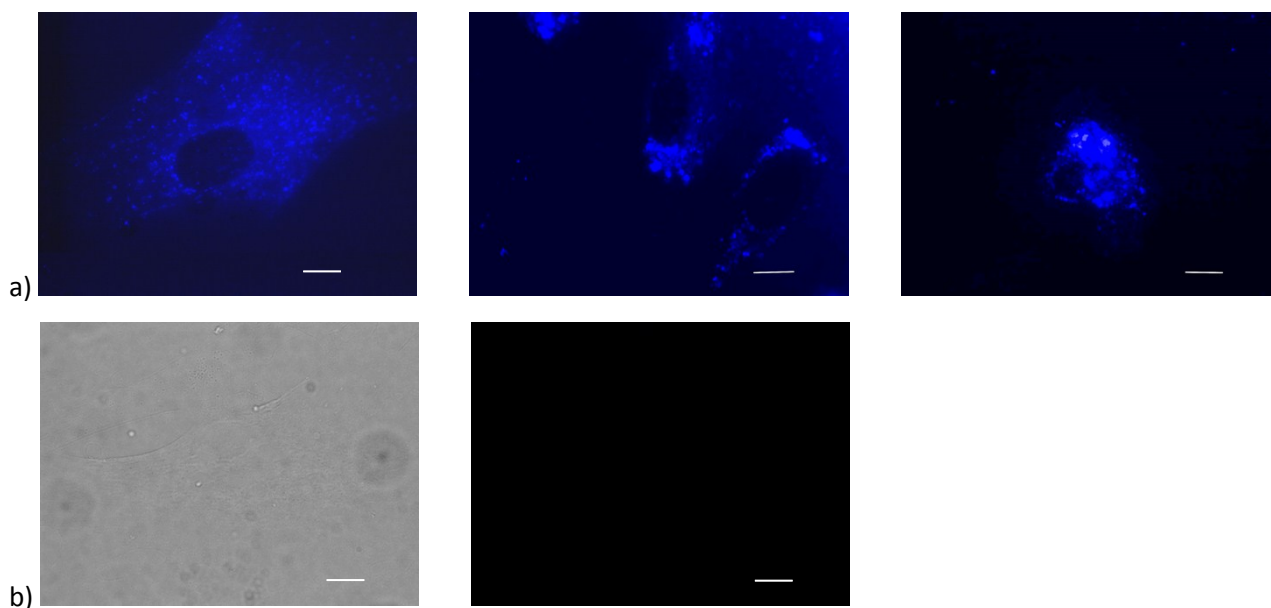


**Figure S14.** a) Fluorescence microscopy images of living primary dermal Fibroblast (left), HUVEC (middle) and macrophages (right) cells incubated with solution of **1** (50  $\mu\text{M}$ ). b) Fluorescence microscopy images of unstained living primary dermal Fibroblast in bright field (left) and with blue filter (right). Scale bar: 10 $\mu\text{m}$ .

## 6. NMR and Mass Spectra

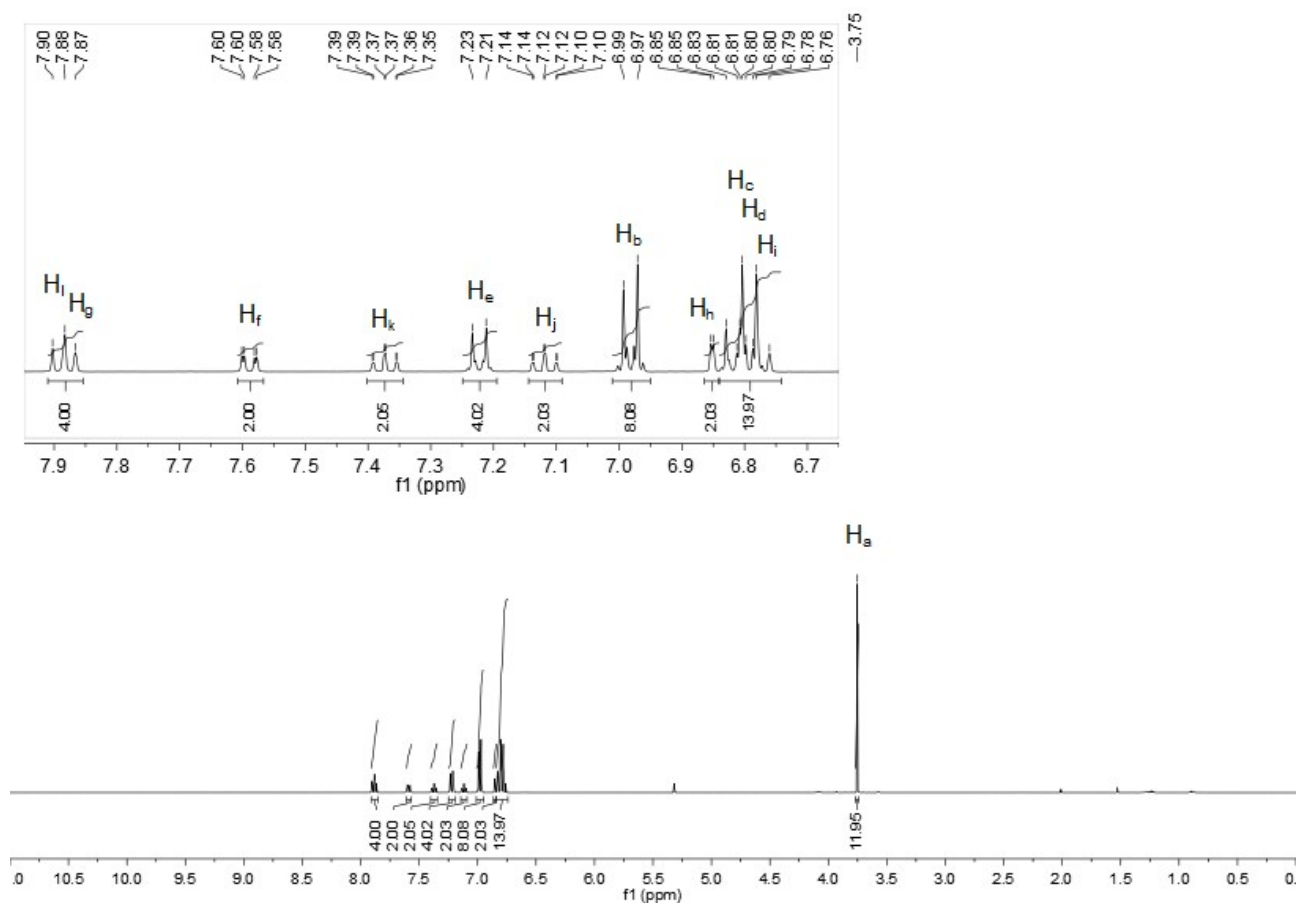


**Figure S15.**  $^1\text{H}$  NMR spectrum of **4**. The symbol \* indicates solvent peak.

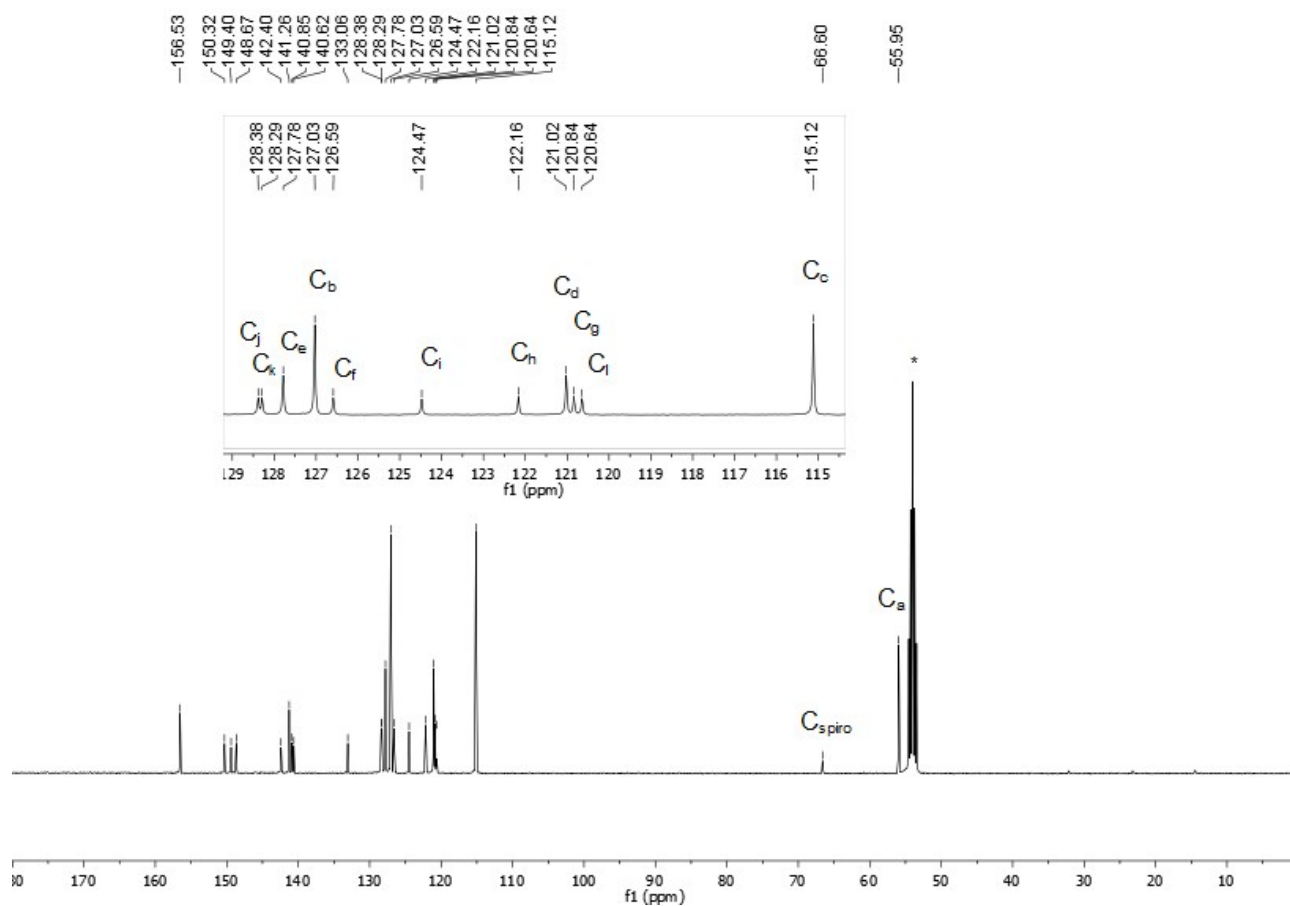


**Figure S16.**  $^{13}\text{C}$  NMR spectrum of **4**. The symbol \* indicates solvent peak.

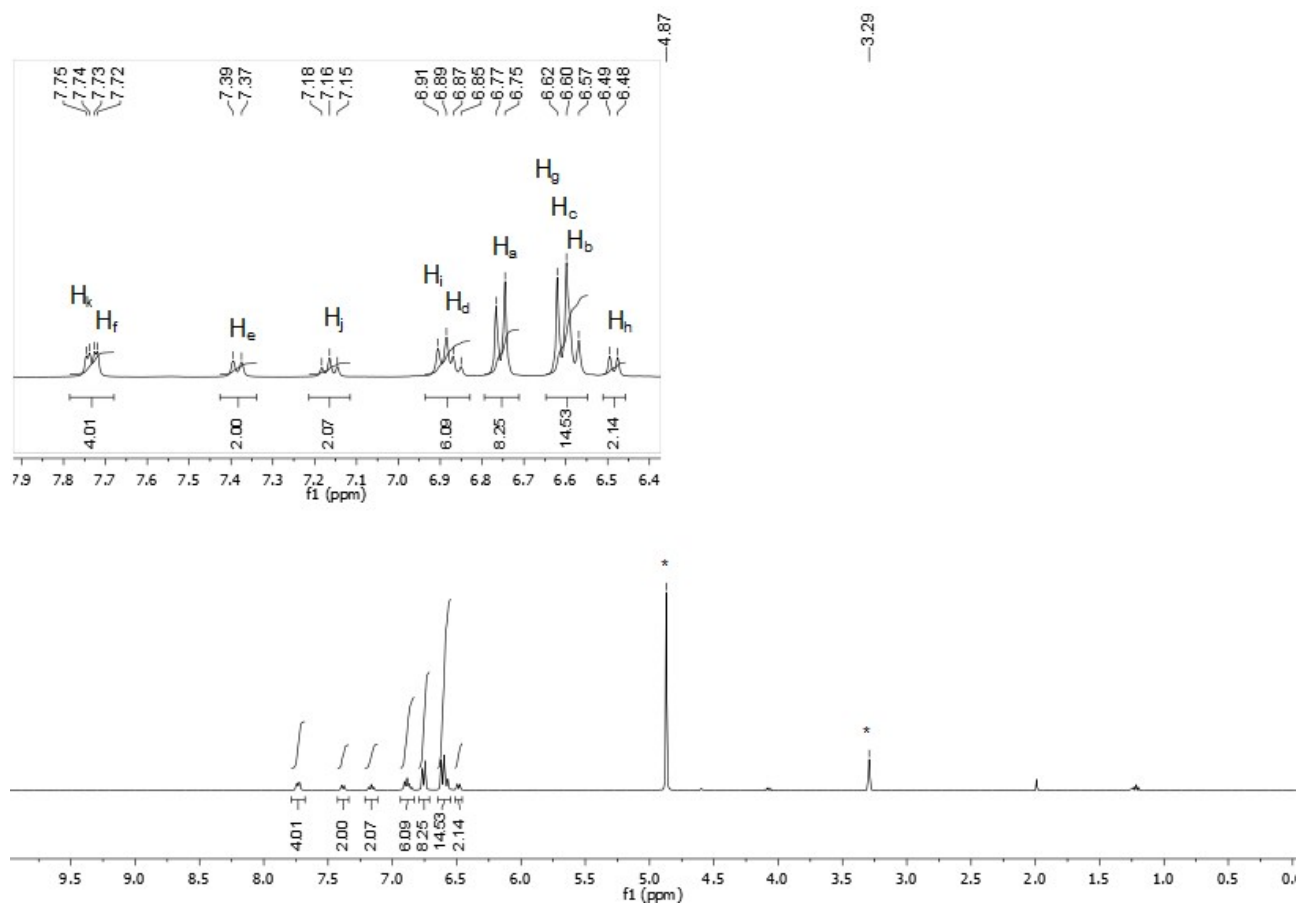


**Figure S17.** <sup>1</sup>H NMR spectrum of **5**. The symbol \* indicates solvent peak.

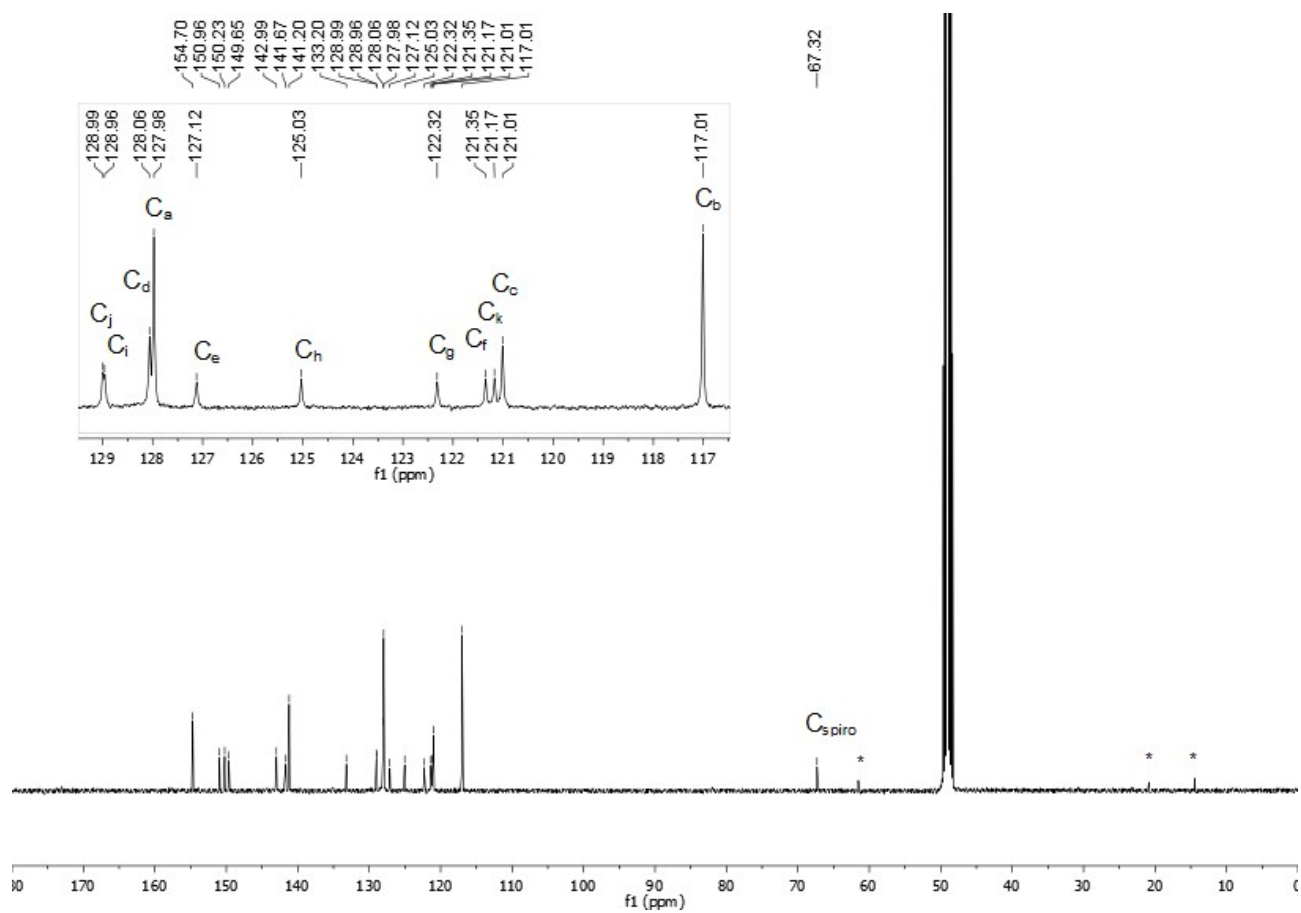


**Figure S18.**  $^{13}\text{C}$  NMR spectrum of **5**. The symbol \* indicates solvent peak.

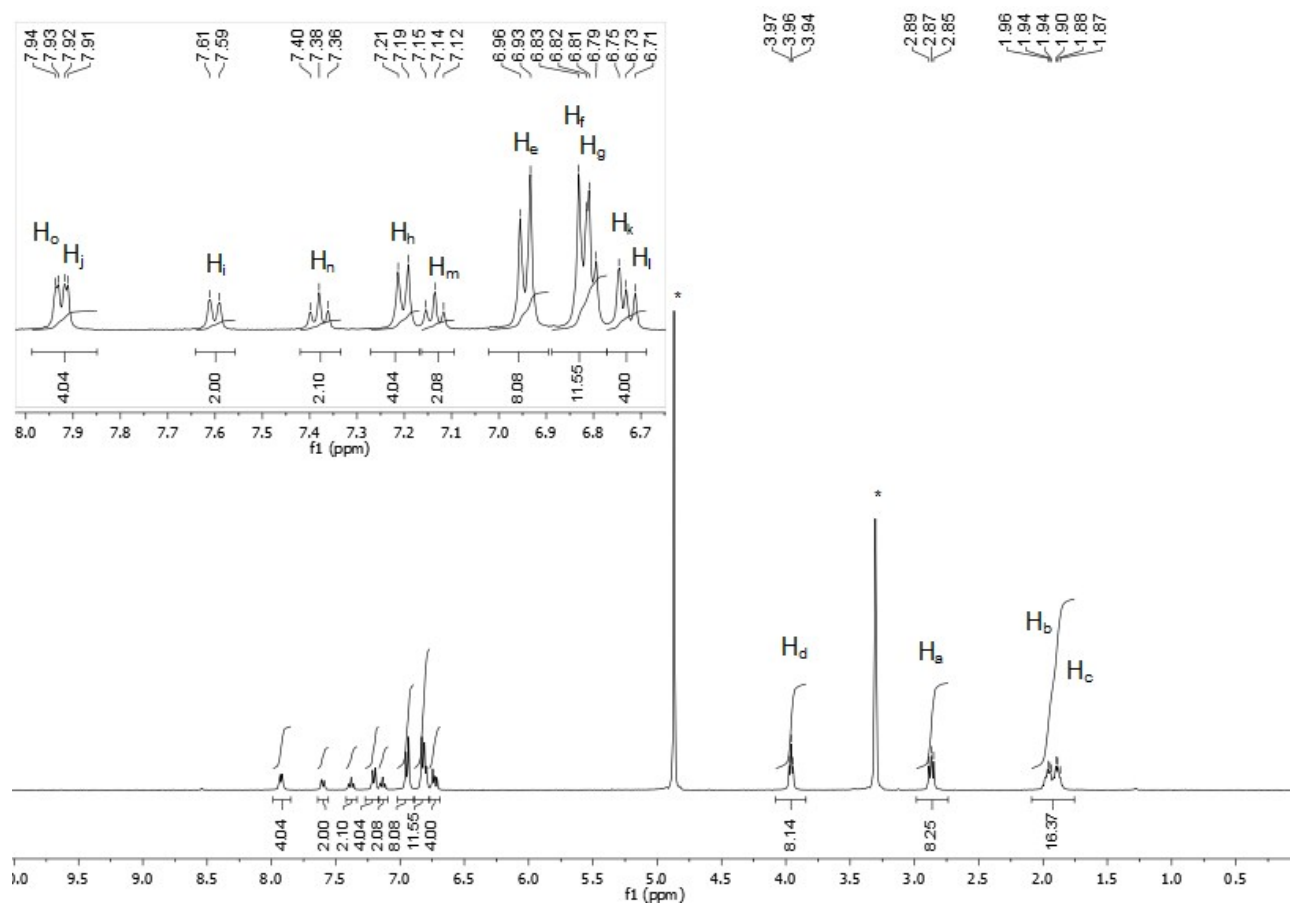


**Figure S19.**  $^1\text{H}$  NMR spectrum of **1**. The symbol \* indicates solvent peak.

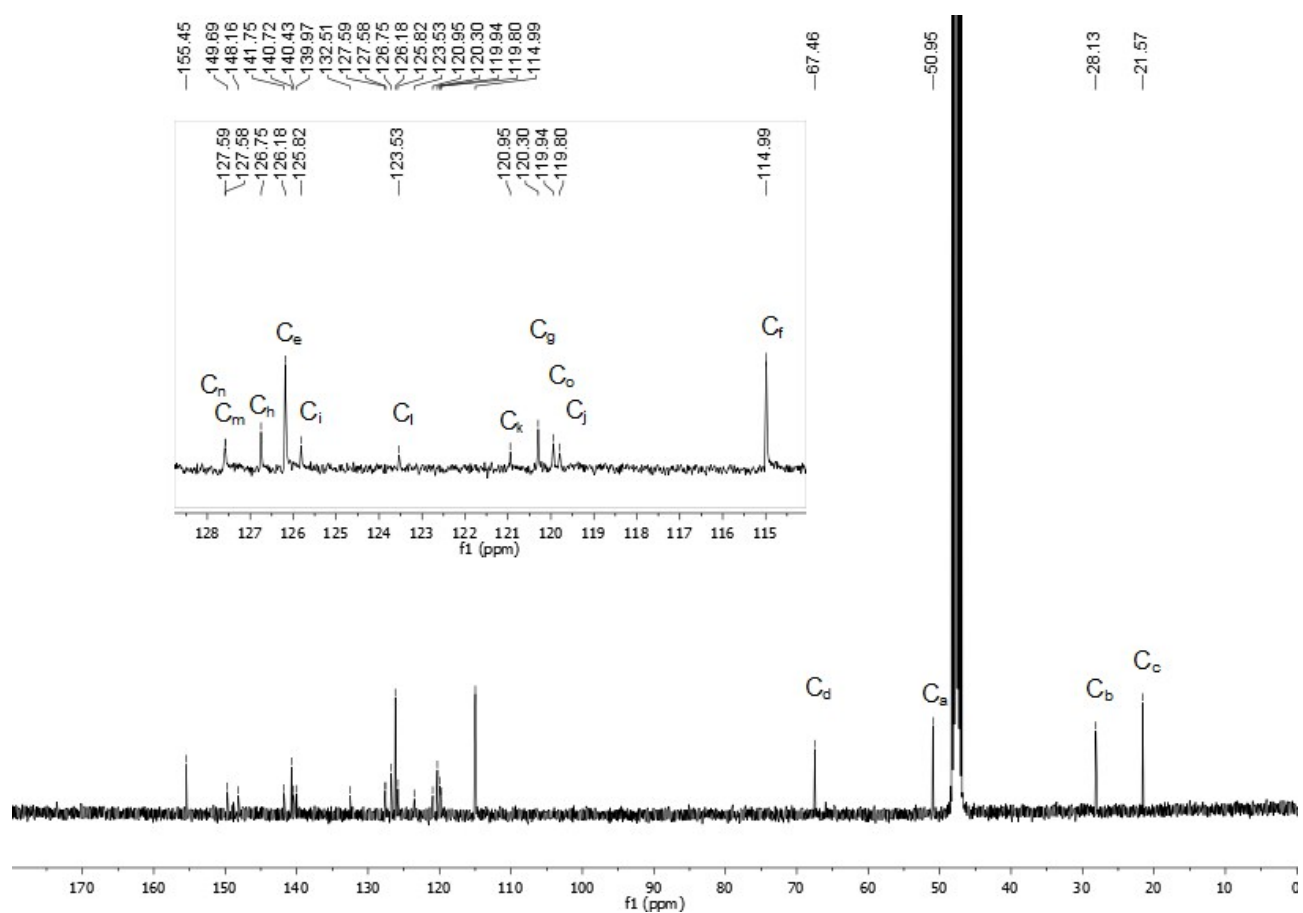


Figure S20.  $^{13}\text{C}$  NMR spectrum of 1.

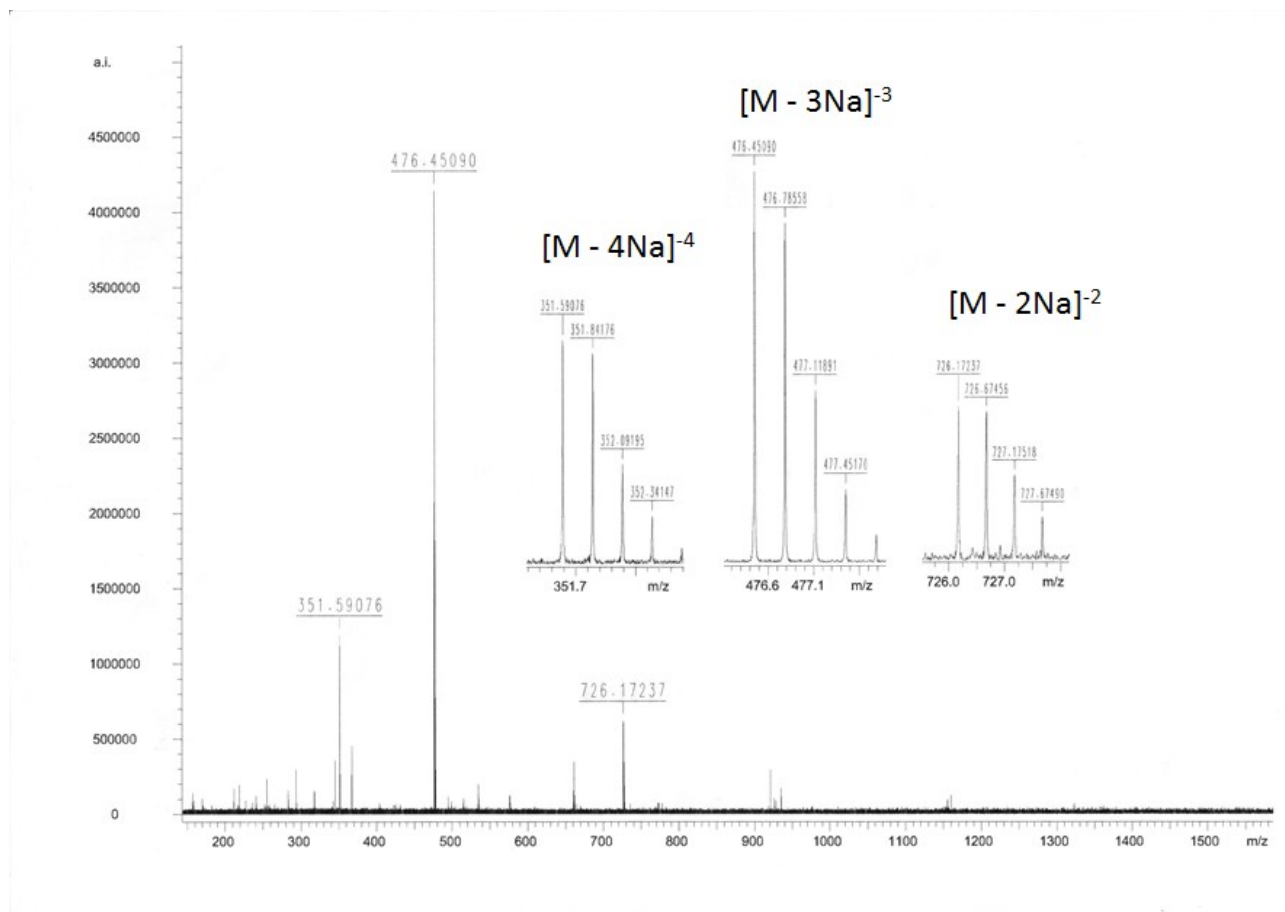


Figure S21. Mass spectrum of 1.

## 7. References

- [S1] Bruker (2013). *APEX2, SAINT and SADABS*: Bruker AXS Inc., Madison, Wisconsin, USA.
- [S2] *SHELXT und SHELXL*: Sheldrick, G. M. *Acta Cryst.*, **2008**, A64, 112.
- [S3] *XP – Interactive molecular graphics, Version 5.1*, Bruker AXS Inc., Madison, Wisconsin, USA, **1998**.
- [S4] Yu, W.-L.; Pei, J.; Huang, W.; Heeger, A. J. *Adv. Mater.* **2000**, 12, 828.
- [S5] Lakowicz, J. R. *Principles of Fluorescence Spectroscopy*, 3<sup>rd</sup> ed., Kluwer Academic/Plenum Publishers, New York, **2006**.
- [S6] Almgren, M.; Grieser, F.; Thomas, J. K. *J. Am. Chem. Soc.* **1979**, 101, 279.